31st Annual International Conference of the IEEE EMBS
Minneapolis, Minnesota, USA, September 2-6, 2009

Shear wave propagation in anisotropic soft tissues and gels

Ravi Namani and Philip V. Bayly

Abstract—**The propagation of shear waves in soft tissue can be visualized by magnetic resonance elastography (MRE) to characterize tissue mechanical properties. Dynamic deformation of brain tissue arising from shear wave propagation may underlie the pathology of blast-induced traumatic brain injury. White matter in the brain, like other biological materials, exhibits a transversely isotropic structure, due to the arrangement of parallel fibers. Appropriate mathematical models and well-characterized experimental systems are needed to understand wave propagation in these structures. In this paper we review the theory behind waves in anisotropic, soft materials, including small-amplitude waves superimposed on finite deformation of a nonlinear hyperelastic material. Some predictions of this theory are confirmed in experimental studies of a soft material with controlled anisotropy: magnetically-aligned fibrin gel.**

I. Introduction

Waves propagate at different speeds in anisotropic soft materials, depending on the direction of propagation, the direction of particle motion, the material orientation, and the stress and strain in the material. Wave propagation in brain tissue is important in magnetic resonance elastography (MRE) [1] and in the brain's response to blast. This paper reviews important results concerning wave propagation in linear and nonlinear materials, and illustrates some of these results with examples from simulation and experiment.

II. Theory

A. Linear theory of waves in transversely isotropic elastic solids

In linear elastic materials, the Cauchy stress tensor **T** is related to the strain tensor, **e**, by the fourth-order elasticity tensor, **C** [2-5]. In Cartesian coordinates this relationship is

$$T_{ij} = C_{ijkl} e_{kl} . \quad (1)$$

The elasticity tensor can be represented by a symmetric matrix of coefficients, D. The relationship between the Cartesian components of C and the elements of D is [2]:

$$C_{ijkl} \to D_{IJ}, \quad \{ij\} \to I, \{kl\} \to J$$
$$\{11\} \to 1, \{22\} \to 2, \{33\} \to 3,$$
$$\{23\} \to 4, \{31\} \to 5, \{12\} \to 6$$

For a transversely isotropic material in which the plane of isotropy is the 2-3 plane, the normal to the plane of isotropy is $\mathbf{a} = \mathbf{e}_1 = [1,0,0]^T$. The corresponding elasticity matrix is:

$$D = \begin{bmatrix} \lambda_p + 2\mu_p & \lambda_m & \lambda_m & & & \\ \lambda_m & \lambda_t + 2\mu_t & \lambda_t & & & \\ \lambda_m & \lambda_t & \lambda_t + 2\mu_t & & & \\ & & & \mu_t & & \\ & & & & \mu_p & \\ & & & & & \mu_p \end{bmatrix} . \quad (2)$$

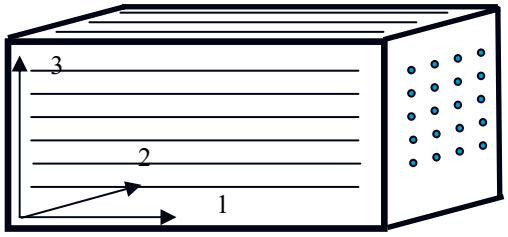

Figure 1: Schematic diagram of a transversely isotropic material with normal to the plane of isotropy (often equivalent to fiber direction) $\mathbf{a} = \mathbf{e}_1 = [1,0,0]^T$.

The elasticity tensor is characterized by five independent parameters $\mu_t, \mu_p, \lambda_t, \lambda_p, \lambda_m$. An alternate set of five independent parameters [3] is given by the two shear moduli μ_t, μ_p, two Young's moduli, E_t, E_p, and a Poisson's ratio ν_{pt} describing the shortening in the plane of isotropy (t-direction) that accompanies lengthening normal to the plane (p-direction). The two sets of five parameters are related by the equations.

$$\nu_{tp} = \frac{E_t}{E_p}\nu_{pt} \quad \text{(Poisson's ratio, t-p)} \quad (3a)$$

$$\nu_{tt} = 1 - \nu_{tp} \quad \text{(Poisson's ratio, t-t)} \quad (3b)$$

$$\mu_t = \frac{E_t}{2(1+\nu_{tt})} \quad \text{(shear modulus, t)} \quad (3c)$$

$$\lambda_p + 2\mu_p = \frac{E_p(\nu_{tt} - 1)}{\nu_{tt} + 2\nu_{pt}\nu_{tp} - 1} \quad (3d)$$

Manuscript received April 23, 2009, 2001. This work was supported by NIH Grant NS055951.

R. Namani is with Washington University, Mechanical, Aerospace, and Structural Engineering, Box 1185, 1 Brookings Drive, St. Louis, Missouri 63130 (phone: 314-935-7562; e-mail: rnamani@seas.wustl.edu).

P.V. Bayly is with Washington University, Mechanical, Aerospace, and Structural Engineering, Box 1185, 1 Brookings Drive, St. Louis, Missouri 63130 USA (e-mail: baylyp@seas.wustl.edu).

$$\lambda_m = \frac{-E_p \nu_{tp}}{\nu_{tt} + 2\nu_{pt}\nu_{tp} - 1} \tag{3e}$$

$$\lambda_t = \frac{E_t(\nu_{tt} + \nu_{pt}\nu_{tp})}{\nu_{tt}^2 + 2\nu_{pt}\nu_{tp} + 2\nu_{pt}\nu_{tp}\nu_{tt} - 1} \tag{3f}$$

Incompressible transversely isotropic material

For an incompressible transversely isotropic material, the Poisson's ratio $\nu_{pt} = 1/2$. In this case, there are only three free parameters [6]. For example, if the two shear moduli μ_t, μ_p, and the ratio of Young's moduli $r_E = E_p / E_t$ are specified, the remaining parameters are:

$$\nu_{tp} = \frac{r_E}{2} \tag{4a}$$

$$\nu_{tt} = 1 - \frac{r_E}{2} \tag{4b}$$

$$E_t = \mu_t(4 - r_E) \tag{4c}$$

$$E_p = r_E \mu_t (4 - r_E) \tag{4d}$$

For an ideally incompressible material the alternate parameters $\lambda_t, \lambda_p, \lambda_m$ are undefined (in practice, for a nearly incompressible material they simply become very large). In incompressible materials, longitudinal waves do not exist, but shear waves propagate with finite speed.

Wave propagation speeds

A propagating plane wave is described by the equation for displacement

$$\begin{aligned} \mathbf{u}(\mathbf{x},t) &= \mathbf{m}\exp[i(k\mathbf{n}\cdot\mathbf{x} - \omega t)] \\ &= \mathbf{m}\exp[i(\mathbf{n}\cdot\mathbf{x} - ct)] \end{aligned} \tag{5}$$

Propagation direction is designated by the unit vector: $\mathbf{n}$ and the "polarization direction" (the direction of particle motion) is specified by the vector $\mathbf{m}$. In longitudinal waves $\mathbf{m} \| \mathbf{n}$; in shear waves $\mathbf{m} \perp \mathbf{n}$. The propagation speed $c = \omega/k$ (m/sec), where k is the wavenumber (rad/m) and ω is the frequency (rad/sec).

Substituting this solution into the equation of motion

$$\mathrm{div}\mathbf{T} = \rho \frac{\partial^2 \mathbf{u}}{\partial t^2} \tag{6}$$

and using (1) the following eigenvalue problem is obtained:

$$C_{ijkl} n_i n_k m_l = \rho c^2 m_j \tag{7a}$$

or

$$\mathbf{Q}(\mathbf{n})\mathbf{m} = \rho c^2 \mathbf{m}. \tag{7b}$$

The Cartesian components of the "acoustic tensor" **Q** are

$$Q_{jl} = C_{ijkl} n_i n_k; \tag{8}$$

they depend on the elasticity tensor **C** and the direction of propagation, **n**. The eigenvalue problem may be solved to find wave propagation speeds and the polarization directions of plane wave solutions.

Example 1: Given a material with elasticity matrix D as in (2). Suppose the normal to the plane of isotropy, **a**, is specified by $\mathbf{a} = \mathbf{e}_1 = [1,0,0]^T$. Let $\mathbf{n} = \mathbf{e}_2 = [0,1,0]^T$ lie in the plane of isotropy. The eigen-speeds and directions are

$$c_1^2 = \frac{\lambda_t + 2\mu_t}{\rho}, \mathbf{m} = [0,1,0]^T \quad \text{(longitudinal)} \tag{9a}$$

$$c_2^2 = \frac{\mu_p}{\rho}, \mathbf{m} = [1,0,0]^T \quad \text{(transverse)} \tag{9b}$$

$$c_3^2 = \frac{\mu_t}{\rho}, \mathbf{m} = [0,0,1]^T \quad \text{(transverse)} \tag{9c}$$

Example 2: Given an elastic material with elasticity matrix D as in (2). Suppose the normal to the plane of isotropy, **a**, is specified. Let **n** be defined only by the angle θ between **n** and **a**. A shear wave solution exists with speed and polarization defined by

$$c^2 = \frac{\mu_p}{\rho}\cos^2\theta + \frac{\mu_t}{\rho}\sin^2\theta, \mathbf{m} \perp \mathbf{n} \tag{10}$$

For materials that are nearly incompressible, the other two eigensolutions (quasi-longitudinal and quasi-shear waves) are of much longer wavelength [2].

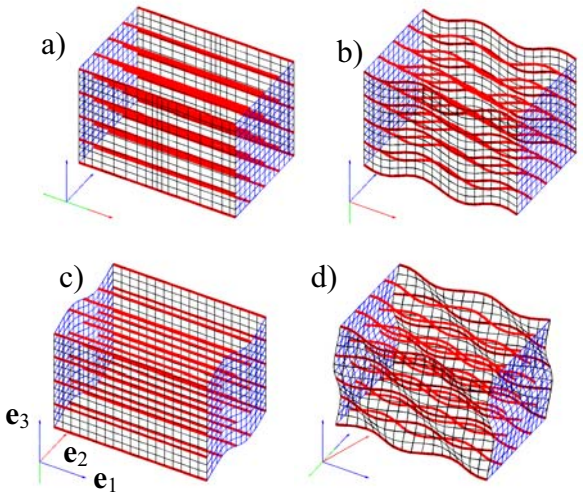

Figure 2: Illustrations of displacement fields due to propagating waves. (a) Longitudinal wave propagating normal to the plane of isotropy (i.e., along the fiber or stretch) direction: $\mathbf{a} = [1,0,0]^T$, $\mathbf{n} = [1,0,0]^T$, $\mathbf{m} = [1,0,0]^T$. (b) Shear wave propagating along the fiber direction, $\mathbf{n} = [1,0,0]^T$, $\mathbf{m} = [0,0,1]^T$. (c) Shear wave propagating transverse to fibers $\mathbf{n} = [0,1,0]^T$, $\mathbf{m} = [0,0,1]^T$. (d) Shear wave propagating in an arbitrary direction relative to **a**: $\mathbf{n} = [1,0,1]^T$, $\mathbf{m} = [0,1,0]^T$. Propagation direction is shown by the red vector; polarization by the green vector.

B. Nonlinear theory: waves in transversely isotropic hyperelastic materials

Biological materials are nonlinear, and may experience considerable residual stress (which is partially or fully relieved when tissue is excised). In these materials, the wave speeds, including directional dependence, are affected by the underlying deformation. Under such conditions, wave propagation is described as infinitesimal motion superimposed on a finite deformation [7-8].

The deformation gradient **F** describes a finite deformation in terms of the relationship between the current position **x** and the reference position **X** of a material element.

$$\mathbf{F} = \frac{\partial \mathbf{x}}{\partial \mathbf{X}} \tag{11}$$

The Lagrangian strain **E** is obtained from

$$\mathbf{E} = \tfrac{1}{2}(\mathbf{F}^T\mathbf{F} - \mathbf{I}) \tag{12}$$

A constitutive law for a hyperelastic material is specified by a strain energy density function, $\hat{W}(\mathbf{E})$; the second Piola-Kirchoff (P-K) stress is:

$$\mathbf{S} = \frac{\partial \hat{W}(\mathbf{E})}{\partial \mathbf{E}} \quad \text{or} \quad S_{AB} = \frac{\partial \hat{W}}{\partial E_{AB}} \tag{13 a, b}$$

The Cauchy stress $\mathbf{T} = J^{-1}\mathbf{F}\mathbf{S}\mathbf{F}^T$ and the first P-K stress $\mathbf{P} = \mathbf{F}\mathbf{S}$.

For small deformations, the nonlinear response can be approximated by a linear relationship using the elasticity tensor [7]

$$c_{ABCD} = \frac{\partial^2 \hat{W}}{\partial E_{AB}\partial E_{CD}} \quad , \tag{14}$$

as in

$$\delta S_{AB} = c_{ABCD}\delta E_{CD} . \tag{15}$$

Now consider the small displacement **u**(**x**,t) superimposed on an initial deformation that maps **X** to **x**. Let the new reference position $\mathbf{X}' = \mathbf{x}$, and the new deformed position $\mathbf{x}' = \mathbf{x} + \mathbf{u}(\mathbf{x},t)$.

The linearized equation of motion with respect to the current configuration is [7]:

$$\mathrm{div}\,\delta\mathbf{T} = \rho\frac{\partial^2 \mathbf{u}}{\partial t^2} \tag{16}$$

The quantity δ**T** is the incremental Cauchy stress due to **u**, which can be written in terms of a new elasticity tensor $\mathbf{A}_0$ and the displacement gradient: $\delta\mathbf{T} = \mathbf{A}_0 grad\mathbf{u}$. In Cartesian coordinates we have

$$\delta T_{ab} = A_{0abcd}\, u_{c,d} \tag{17a}$$

Where the elasticity tensor $\mathbf{A}_0$ in Cartesian coordinates:

$$A_{0abcd} = T_{bd}\,\delta_{ac} + L_{0abcd} \quad , \tag{17b}$$

the Cauchy stress due to the finite deformation is

$$T_{bd} = J^{-1}F_{bB}F_{dD}S_{BD} \quad , \tag{17c}$$

and

$$L_{0abcd} = J^{-1}F_{aM}F_{bB}F_{cP}F_{dD}c_{MBPD} \quad . \tag{17d}$$

Substituting (17) into (16) we obtain the linearized equation governing wave propagation,

$$\frac{\partial}{\partial x_a}[A_{0abcd}u_{c,d}] = \rho\frac{\partial^2 u_b}{\partial t^2} \quad . \tag{18}$$

It is apparent that the initial deformation affects the elasticity, even inducing effective anisotropy into the equations for wave propagation.

Example 3: Incompressible, isotropic material, stretched

Given a neohookean, incompressible material that has undergone uniaxial stretch (Fig. 3). Wave propagation speeds depend on the stretch and the direction of propagation [8].

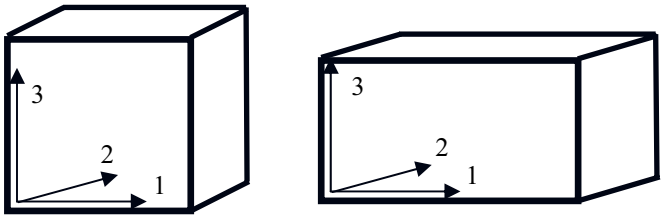

Figure 3: Schematic diagram of finite uniaxial stretch.

The constitutive model is given by

$$W = \frac{\mu}{2}(I_1 - 3), \quad J = \det F = 1 \tag{19}$$

Suppose the material undergoes normal stretches $\lambda_1, \lambda_2,$ and λ_3 ($\lambda_1\lambda_2\lambda_3 = 1$). The elasticity tensor $\mathbf{A}_0$ is formed, as described above, and a plane wave solution (as in Eq. 5) is assumed. Again, we obtain an eigenvalue problem (as in Eq. 7), where (in Cartesian coordinates):

$$Q_{jl} = A_{0ijkl}\, n_i n_k \tag{20}$$

For this general situation, shear wave speeds are [8]

$$c_{2,3}^2 = \frac{\mu}{\rho}(\lambda_1^2 n_1^2 + \lambda_2^2 n_2^2 + \lambda_3^2 n_3^2), \mathbf{m} \perp \mathbf{n} . \tag{21}$$

Longitudinal waves do not exist if the material is incompressible.

For the case of uniaxial stretch λ_1, wave propagation parallel to direction of stretch is specified by setting

$\mathbf{n} = [1,0,0]^T$. The corresponding wave speed is

$$c_{2,3}^2 = \frac{\lambda_1^2 \mu}{\rho}, \mathbf{m} = [0, m_2, m_3]^T \qquad (22)$$

Propagation perpendicular to stretch is specified by setting $\mathbf{n} = [0,1,0]^T$; in this case the propagation speed is

$$c^2 = \frac{\lambda_2^2 \mu}{\rho} = \frac{\mu}{\lambda_1 \rho} \qquad (23)$$

Example 4: Transversely isotropic hyperelastic material

A transversely isotropic material is symmetric with respect to the normal to the plane of isotropy: **a** [6]. The quantities $I_4 = \mathbf{a}^T \mathbf{C} \mathbf{a}$ and $I_5 = \mathbf{a}^T \mathbf{C}^2 \mathbf{a}$ are "pseudo-invariants" (invariant under rotations about **a**). I_4 is equivalent to the stretch λ_a in the direction of **a**, whereas I_5 includes contributions from shear out of the plane of isotropy (in Cartesian coordinates these correspond to the strain components $E_{12}, E_{13}, E_{21}, E_{31}$), as well as stretch λ_a . The vector **a** typically reflects the direction of fibers, or other structural anisotropy. A simple constitutive law for a hyperelastic material that illustrates anisotropy in shear is

$$W = \frac{\mu}{2}\left(\bar{I}_1 - 3\right) + \frac{k_3}{2}\left(I_5 - I_4^2\right) + \frac{\kappa}{2}\left(J-1\right)^2 \qquad (24)$$

The intuitive prediction that wave speed will depend on the polarization of the shear wave can be confirmed. For example, suppose $\mathbf{a} = \mathbf{e}_1 = [1,0,0]^T$. For propagation perpendicular to fibers ($\mathbf{n} \perp \mathbf{a}$) there are two possible shear wave speeds, as well as a longitudinal wave speed.

$$c_1^2 = \frac{\frac{4}{3}\mu + \kappa}{\rho}, \mathbf{m} \| \mathbf{n} \qquad \text{(longitudinal)} \quad (25a)$$

$$c_2^2 = \frac{\mu + k_3}{\rho}, \mathbf{m} = [1,0,0]^T \qquad \text{(out-of-plane shear)} (25b)$$

$$c_3^2 = \frac{\mu}{\rho}, \mathbf{m} = [0,0,1]^T \qquad \text{(in-plane shear)} \quad (25c)$$

Note that the shear wave solution involving only deformation in the plane of isotropy is not affected by anisotropic term in the constitutive equation.

All the preceding results are valid in an infinite domain, with no dissipation. Surface interactions and energy loss will affect the solutions observed in bounded, physical systems.

III. SIMULATION

Simulations were performed to visualize wave propagation in anisotropic soft materials, and to explore the effects of boundary conditions (finite domain) and dissipation. A cube of material, 25 mm on a side, was modeled and simulated using COMSOL finite element software (COMSOL, Burlington, MA). The domain was discretized into 16,985 tetrahedral elements (Lagrange quadratic type). Normal displacements on five sides were zero, and on the sixth side (top) a distributed harmonic force was applied in the x-direction. For all the examples shown, the frequency was 400 Hz. Since the material is linear the wavelength is independent of amplitude. Dissipation is modeled by a loss factor, γ , where ($\sigma_0 e^{i\omega t} = \mu(1+i\gamma)\varepsilon_0 e^{i\omega t}$). Dissipation is necessary to obtain converged solutions; the value of the loss factor was chosen to model experimental behavior (Fig. 7). The frequency response was obtained via the PARDISO linear system solver (tolerance = 1.0×10^{-6}).

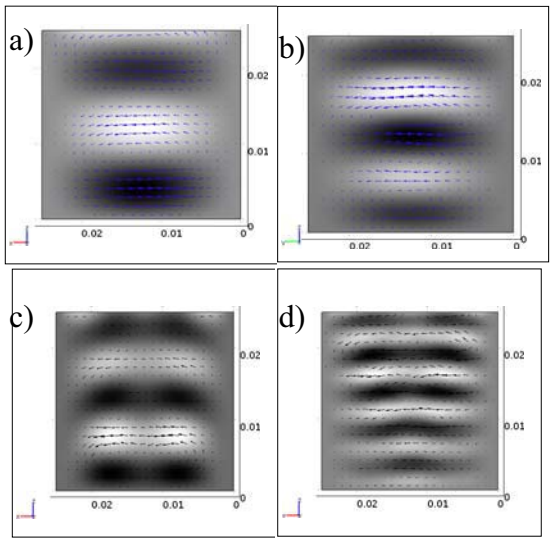

Figure 4: Displacement images during shear wave propagation in transversely isotropic materials at a frequency of 400Hz. (Left) Excitation normal to the plane of isotropy; (Right) Excitation in the plane of isotropy. Parameters: (a),(b) Anisotropy ratio of Young' moduli: r_E=2, in-plane shear modulus μ_t=860 Pa, out of plane shear modulus μ_p=2000 Pa; (c), (d) r_E=2, μ_t=215 Pa, μ_p=1000 Pa. Loss factor $\gamma = 0.1$. The Poisson's ratio was set to $\nu_{pt} = 0.49$.

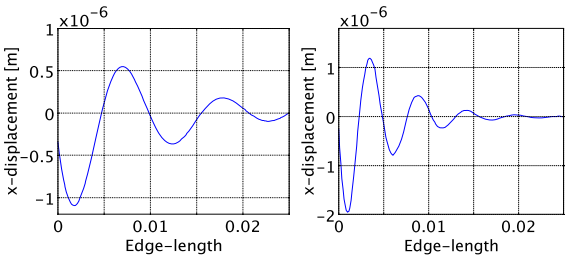

Figure 5: Cross-sectional plot of displacement due to propagating shear waves. Parameters: r_E=2, μ_t=215 Pa, μ_p=1000 Pa. Loss factor $\gamma = 0.5$.

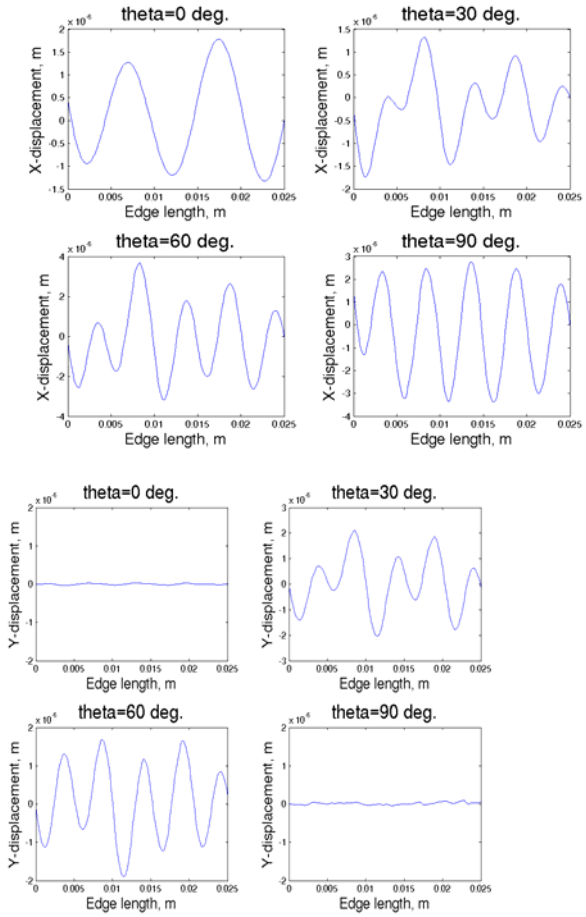

Figure 6: Simulation: Displacements parallel (x) and perpendicular to (y) the direction of excitation, shown for fiber orientations of 0º, 30 º, 60 º, and 90 º. Results show more than one wave speed for directions other than 0º and 90º; the combination of material anisotropy and reflective boundary conditions leads to interaction of shear waves of different speeds and directions.

IV. EXPERIMENTAL EXAMPLES

Fibrin gels with anisotropic structure and mechanical properties can be obtained by polymerization in a strong magnetic field [9-10]. MRE of aligned fibrin gel illustrates features of shear wave propagation in anisotropic materials.

Human plasminogen-free fibrinogen (EMD Biosciences, La Jolla, CA, product no. 341578) was dissolved in tris-buffered saline (TBS) and dialyzed in TBS overnight in polymer tubing (Thermo Scientific, Rockford, IL, product no. 68700, 8,000 MWCO). The fibrinogen solution was filtered with a 5 μm filter. Equal volumes of fibrinogen and thrombin (Sigma-Aldrich, St. Louis, MO, product no. T4648) solutions were mixed with $CaCl_2$ solution yielding the final concentrations: 10 mg/mL fibrinogen, 25 mM Ca^{++}, and 0.2 NIH units/mL thrombin. The solution was poured into a 20 mm x 20 mm x 20 mm hollow plastic cube. Further details are in [10].

Gels were polymerized for 2hrs at room temperature (24ºC) in the center of the bore of an 11.7T MRI scanner (Varian, Inc., Palo Alto, CA). The direction of the magnetic field during polymerization, denoted by the unit vector $\mathbf{e}_B$ was recorded and marked on each sample.

MRE was performed in a 4.7T magnet (Oxford Instruments, Oxfordshire, UK) with a Varian imaging system (Varian Inc., Palo Alto, CA). A piezoelectric actuator (Model APA100M-NM, CEDRAT Technologies, Troy, NY) was attached with the cube to a rigid plastic base. The actuator arm was coupled to the surface of the gel in order to excite shear motion at 400Hz in either of two directions, depending on the orientation of the cube. The actuator and gel assembly was placed in the transmit/receive coil of the scanner, and a standard spin-echo sequence, modified to include motion encoding gradients [1], was used to acquire images. First, the actuator was excited to provide surface displacements in the direction of $\mathbf{e}_B$ (i.e., parallel to the axis of the sample that was aligned with the magnetic field when the gel was polymerized). Second, the specimen was rotated by 90º so that the actuator provided surface displacements in the direction normal to $\mathbf{e}_B$.

Standard MRE procedures were used to visualize wave motion. MRI data obtained during wave propagation were Fourier-transformed into the spatial (image) domain, normalized with respect to the baseline image, and phase-unwrapped (PhaseVisionTM, Loughborough, UK) to remove the 2π phase ambiguity, resulting in a phase-contrast image (Fig. 7a, 7c) with intensity proportional to displacement.

In Figure 7, the wave length depends on the direction of excitation relative to the direction of the magnetic field during polymerization. This is consistent with the alignment of fibrin fibers with the magnetic field observed in [9-10], and accompanying anisotropy in shear modulus [10].

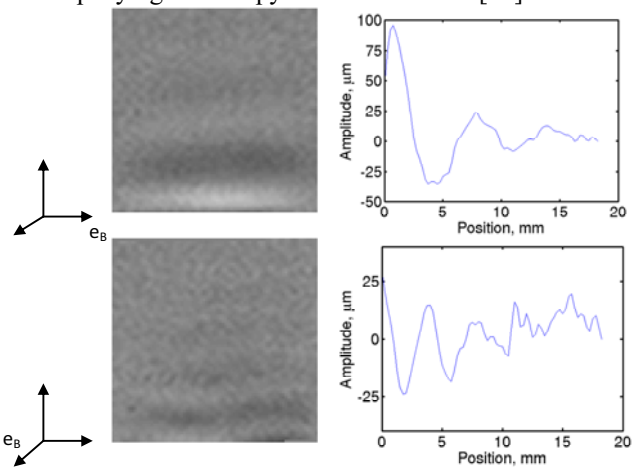

Figure 7: MR Images of propagating shear waves in anisotropic fibrin gels polymerized in a magnetic field. (Top) Excitation parallel to the direction of imposed magnetic field (dominant fibrin fiber direction); (Bottom) Excitation perpendicular to the dominant fiber direction. (Right) Cross-sectional plots of displacement (c.f. Fig. 5).

V. DISCUSSION

This paper reviews theoretical results on shear waves in anisotropic elastic and hyperelastic materials. A particularly interesting result is that a finite static deformation, such as a stretch, affects the propagation of superimposed shear waves. In effect, the stretch can mimic the effect of structural anisotropy. We have recently observed that white matter is under measurable tension along the axis of fiber tracts [11]. This may confound the measurement of mechanical properties by MRE.

Viscoelastic effects are clearly important in soft tissues. Dissipative effects limit the penetration depth of waves in MRE [1]. The magnitude of shear modulus is significantly greater at high frequencies [12]. Viscoelasticity is not simple to model, and the choice of model affects results. In this paper, we use a "loss modulus" to introduce dissipation into our finite element model.

Sinkus et al. [13] describe an approach to estimation of the shear moduli μ_t, and μ_p, given MRE measurements of experimental displacement fields. Such fields generally include motion other than shear waves. Their method also provides estimates of a viscous parameter [14]. A key feature of their method is the use of the Hodge-Helmholtz decomposition to eliminate contributions of longitudinal waves, and focus on shear wave contributions.

Experimental measurements of shear wave propagation in an anisotropic gel are consistent with predictions from a linear model. Specifically, the wavelength is longer for shear waves polarized along the dominant fiber direction than in a direction perpendicular to the fibers. Simulations also exhibit this behavior, when excitation is parallel or normal to the plane of isotropy. When the excitation is at an arbitrary angle, simulations illustrate the complexity of wave propagation: solutions do not consist of a single wave propagating in a single direction. Rather, displacement fields consist of a superposition of waves propagating in different directions, reflecting off boundaries and surfaces.

In this paper, the experiments have guided simulations. Excitation at 400 Hz produces waves that propagate through fibrin gel with several wavelengths visible in our samples; the same frequency was used in simulation. Also, since fibrin gels and tissues are nearly incompressible, a Poisson's ratio $\nu_{pt} = 0.49$ was used. If the gels deviate from incompressibility ($\nu_{pt} = 1/2$,), longitudinal waves exist but are are extremely long, and interaction between longitudinal and transverse waves can exist. The effect of pre-stress may be important in modeling brain injury, since white matter has been observed to be under measurable tension in mammalian brain tissue [11]. This tension appears to be of the same order of magnitude as the linear shear modulus, so it may affect shear wave propagation patterns.

In conclusion, the effects of anisotropy, finite deformations, and boundary conditions complicate the interpretation of shear wave measurements, and the prediction of the response to transient excitation, such as blast. Experimental results in materials with controlled anisotropy are possible and will help illuminate the behavior of brain tissue.

REFERENCES

[1] R. Muthupillai, D.J. Lomas,P.J. Rossman, J.F. Greenleaf, A. Manduca, R.L. Ehman, R. L., 1995. Magnetic resonance elastography by direct visualization of propagating acoustic strain waves. Science, 1995, vol. 5232, pp. 1854-1857.

[2] C. Chapman, *Fundamentals of Seismic Wave Propagation*, Cambridge: Cambridge University Press, 2004.

[3] J.P. Marquez, G.M. Genin, E. L. Elson, "On the application of strain factors for approximation of the contribution of anisotropic cells to the mechanics of a tissue construct," Journal of Biomechanics, 2006, vol. 39, pp. 2145-2151.

[4] R.M. Jones, *Mechanics of Composite Materials* (2nd ed), London: Taylor and Francis, 1999.

[5] D.F. Parker, "Elastic wave propagation in strongly anisotropic solids," in *Continuum Theory of the Mechanics of Fibre-Reinforced Composites*, A.J.M. Spencer, Ed. New York: Springer-Verlag, 1984, pp. 217-244.

[6] A.J.M. Spencer, "Constitutive theory for strongly anisotropic solids," in *Continuum Theory of the Mechanics of Fibre-Reinforced Composites*, A.J.M. Spencer, Ed. New York: Springer-Verlag, 1984, pp. 1-32.

[7] P. Chadwick and R.W. Ogden, "On the definition of elastic moduli," Arch Rational Mech Anal , 1971, vol. 44, pp. 41-53.

[8] P. Chadwick and R.W. Ogden, "A theorem of tensor calculus and its application to isotropic elasticity," Arch Rational Mech Anal , 1971, vol. 44, pp. 54-68.

[9] N. Dubey, P.C. Letourneau, R.T. Tranquillo. Neuronal contact guidance in magnetically aligned fibrin gels: effect of variation in gel mechano-structural properties. Biomaterials, 2001, vol. 10, pp. 1065-1075.

[10] R. Namani, M. Wood, S. E. Sakiyama-Elbert, P. V. Bayly, "Anisotropic mechanical properties of magnetically aligned fibrin gels measured by magnetic resonance elastography," ASME Summer Bioengineering Conference, Lake Tahoe, CA, 2009.

[11] G. Xu, P.V. Bayly, L.A. Taber, "Residual stress in the adult mouse brain," Biomech Model Mechanobiol (in press).

[12] S.M. Atay, C. Kroenke, A. Sabet, P.V. Bayly , Measurement of the dynamic shear modulus of mouse brain tissue in vivo by magnetic resonance elastography. Journal of Biomechanical Engineering, 2008 vol. 130, pp. 021013.

[13] R. Sinkus, M. Tanter, S. Catheline, J. Lorenzen, C. Kuhl, E. Sondermann, and M. Fink. Imaging anisotropic and viscous properties of breast tissue by magnetic resonance elastography. Mag Res Med, 2005, vol. 53, pp. 372-387.